



(RESEARCH ARTICLE)



Automated potholes detection using vibration and vision-based techniques

Vyas Toral ^{1,*}, Tandel Krushangi ² and Varia Harishkumar R. ³

¹ Gujarat Technological University, Ahmedabad 382424, Gujarat, India.

² L. D. College of Engineering, Ahmedabad 380015, Gujarat, India.

³ Adani Institute of Infrastructure Engineering, Ahmedabad 382421, Gujarat, India.

World Journal of Advanced Engineering Technology and Sciences, 2023, 10(01), 157–176

Publication history: Received on 02 September 2023; revised on 12 October 2023; accepted on 14 October 2023

Article DOI: <https://doi.org/10.30574/wjaets.2023.10.1.0276>

Abstract

Roads serve as vital parts of our infrastructure, providing as crucial conduits for people's mobility and connectivity. However, the growing number of vehicles on the road has resulted in an increase in pavement strain and degradation, which has a substantial impact on the entire riding experience. To achieve a high-quality surface, roadways must be consistently monitored and maintained.

In recent years, transportation infrastructure agencies and governments have shown a rising interest in leveraging new technologies to monitor road pavements. This interest derives from the difficult and time-consuming nature of manual and instrumented techniques. Automated technologies have arisen as a response to these issues, notably in recognizing pavement deterioration, such as the common problem of potholes.

The objective of this research is to identify potholes using two low-cost automated techniques: a vibration-based method that uses the G-Sensor Logger application and a vision-based way that uses image processing. On the same roads, both approaches were employed and compared, with manual surveying utilized to validate the results. The results showed that vision-based strategies were more effective than vibration-based methods.

Finally, although vibration-based analysis is appropriate for routine monitoring, vision-based analysis provides a more comprehensive and in-depth examination of road conditions. These discoveries will help future efforts to better monitor and maintain road surfaces, ensuring a smooth and safe travel experience for everybody.

Keywords: Infrastructure; Pavement distress; Road surface quality; Pothole detection; Road quality assessment

1. Introduction

Detecting pavement deterioration is crucial because it immediately affects the safety and comfort of road users while also improving the effectiveness of road maintenance. Traditionally, inspectors travelled the highways to assess the severity of the problems when it comes to pavement distress detection and analysis. These manual methods are difficult, subjective, expensive, time-consuming, and prone to human error, among other problems.

To overcome these challenges, transportation organizations and researchers globally have shifted towards automated methods for pavement distress detection. Technologies like Ground Penetrating Radar, Laser Road Imaging Systems, video/image processing, and smartphone sensors have gained traction. Among these, smartphone sensors and video processing have gained significant popularity due to their ease of use and cost-effectiveness. Unlike more complex methods that necessitate specialized equipment like lights and lasers, smartphone sensors and video processing provide a more accessible and affordable alternative for surveying road conditions.

* Corresponding author: Vyas Toral.

1.1. Road Pavement Distress: Pothole

Potholes are concave deformations that vary in size and display a bowl-like shape in the bituminous surface or that extend into the binder/base course. These formations result from the pavement materials' localized disintegration. Figure-1 shows severity of potholes.



Figure 1 Photos of Different Severity of Potholes

1.2. Causes

Potholes are primarily caused by compromised bituminous wearing coat adhesion brought on by water infiltration or expanded surface voids. Due to the impact of the traffic and the loss of cohesiveness, the pavement softens. Plastic filler in the granular base may speed up pothole formation. If surface aggregates are not properly maintained, they may become looser over time and contribute to potholes. Additionally, there may be contributing factors such as insufficient bitumen content in certain areas of the surfacing layer or poor compatibility with the underlying water-bound macadam foundation layer. Potholes can result from a lack of bitumen, especially when combined with poor camber and a thin bituminous surface. In densely graded mixtures, imbalanced fines and penalties can also cause potholes.

Potholes are categorized into three sizes: small, medium, and large. A small pothole measures 25 mm deep and 200 mm wide.

1.3. Severity

A medium pothole ranges from 25 to 50 mm in depth and 500 mm in width. Large potholes are more than 50 mm deep and 500 mm wide.

1.4. How to Measure/Measurement

At each severity level, note the quantity of potholes and the square meters of the area that they have affected. The lowest point beneath the pavement's surface determines the pothole depth. The fatigue cracking area is modified as necessary when a pothole develops within it. A pothole's minimum plan dimension is roughly 0.02 m². On distress map sheets, it is essential to note the precise plan dimensions and pothole area. While they should not be included in the measurement summaries, potholes that don't meet the minimum plan dimension should be noted and marked on the distress map sheets.

2. Literature Review

Pavement monitoring techniques can be broadly categorized into static and dynamic methods, based on how vibration data is collected. Dynamic pavement monitoring has gained traction, influenced by factors such as equipment availability, pavement type (asphalt, concrete, or composite), and road classification.

One effective method for pavement distress detection is vision-based analysis, which involves capturing video footage of the road surface. Lekshmi et al. (2020) successfully utilized this approach to detect cracks, potholes, and patches with an impressive 84% accuracy. Similarly, Zhang et al. (2021) employed deep neural networks to identify and classify pavement distress, leveraging a specialized dataset to train and evaluate Convolutional Neural Networks (CNNs) with diverse topologies and layer combinations.

To comprehensively evaluate pavement conditions, the Pavement Performance Index (PPI) is computed by summing the product of deterioration parameters' ratings and respective weightages. Issa et al. (2021) proposed an artificial

intelligence-driven method for predicting the Pavement Condition Index (PCI). This involved gathering distress data through visual inspections, forming a database, and subsequently employing an Artificial Neural Network (ANN) model for accurate PCI predictions.

In the context of pavement quality assessment, Sinha and Hagawane (2020) devised a formula using IRC and ASTM techniques to rate pavement quality across an 80-kilometer four-lane flexible pavement stretch. Their study compared ratings obtained from both methods to ascertain correlations, accuracy, and precision in the results. Additionally, Jain et al. (2013) applied artificial neural networks (ANN) to analyze the present serviceability index (PSI) for flexible pavements on urban highways. Their findings demonstrated that the ANN model outperformed traditional regression models, showcasing higher R2 values and improved error metrics.

3. Methodology and Study Area

The methodology for this study is shown in Figure 2, which outlines a systematic approach to achieving the study's goals. Problem identification is the first step, which is then followed by a thorough literature review to determine the goals and objectives of the study. The study used three different methods for data collection from road surfaces, which was essential to achieving its objectives.

The road surface data was collected using an Android application called G-sensor logger in the vibration-based method. In the case of the manual distress surveying technique, data was gathered by visually observing the road surface, whereas for the vision-based approach, photographs of the road surface were taken. The busy coastal highway Bhimpore, which is well-known for its significant distress, served as the site of the data collection.

Excel was used to process the data, create graphs that show the acceleration data, and analyse the vibration-based data. The quantity of potholes present might be predicted thanks to these graphs. On the other hand, a Convolutional Neural Network (CNN) technique was used to detect potholes using photographs for the vision-based data. Five road segments were subjected to both methods, and manual surveying was used to confirm the findings. A comparison study of the two techniques was done to determine the pothole detection's accuracy. A thorough analysis of the results from both techniques resulted in a definitive judgement. Figure 3 shows schematic diagram of study approach.

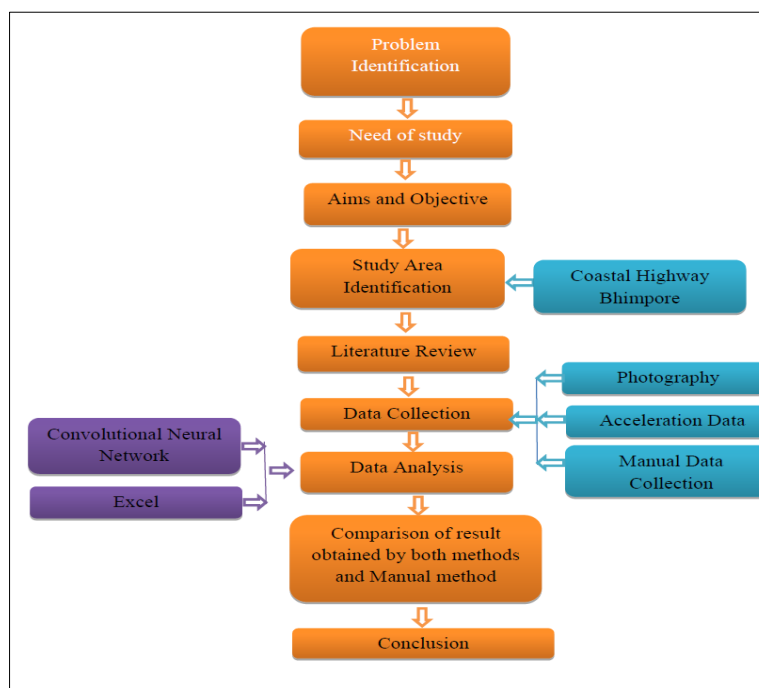


Figure 2 Flow Chart of Methodology

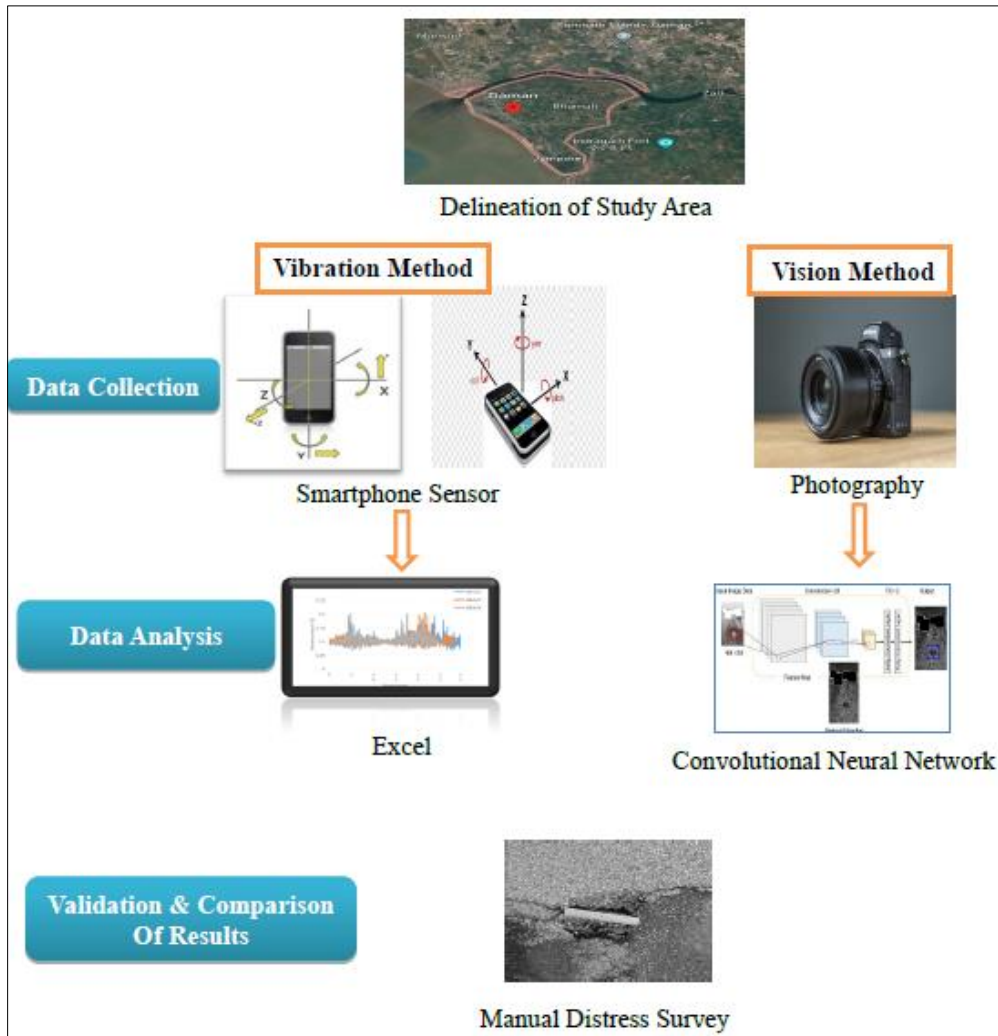


Figure 3 Schematic diagram of study approach

Daman is a developing Union Territory in India that is positioned between Gujarat and Maharashtra. It has evolved into a desirable hub for a number of industries over time, luring them to the area to establish their presence. Daman is also well-known for being a top tourist attraction, with a sizable influx of visitors every day, particularly on weekends. This influx has resulted in an increase in commercial and industrial traffic, which has had a considerable influence on the state of the roadways.

The Coastal Highway Bhipore, a crucial section of National Highway 848B, is extremely significant since it connects Daman with the checkpoint for entry and exit. Being accessible to a wide variety of vehicles, it is one of Daman's busiest highways. This road receives heavy traffic and as a result has seen a considerable decline in quality. The road's poor condition is made worse by the fact that it is particularly pothole-ridden during the rainy season. This road was therefore selected as the study region to concentrate on the detection of these common potholes. Figure-4 shows details of study area.



Coastal Highway Bhimpore	
Area Sq. Km	72
Density per Sq. Km	2655
Elevation	5m (16 ft.)
Time zone	UTC+5:30 (IST)
Coordinates	20.41°N 72.89°E
Government Type	Daman Municipal Council



Figure 4 Details of Study Area

The Daman Ganga River divides Daman into two distinct regions known as Nani-Daman and Moti-Daman. Contrary to its name, Nani-Daman is the larger area, and it is home to important institutions like important hospitals, supermarkets, and residential neighborhoods. On the other hand, Moti-Daman, where the majority of the administrative offices are located, is where the old city is predominantly located.

4. Basic of Different Pothole Monitoring Techniques

4.1. Vision based Pothole Detection Technique

This method uses the CNN algorithm to locate and detect potholes in asphalt pavements. This technique has many benefits, such as automated feature extraction processes and consistent accuracy under various settings. The proposed method successfully recognises and detects potholes with high accuracy and robustness. With results that serve as a strong foundation for efficient pavement maintenance, it has the potential to autonomously replace conventional manual pavement inspection methods.

4.2. Convolutional Neural Network

The term "Artificial Intelligence" has enormous relevance in the field of computer technology and has completely changed the way we live our daily lives by making a variety of activities easier. These innovations, which have immensely helped humanity, are designed to reduce human labor. Amazing progress has been achieved in bridging the gap between human and machine capabilities thanks to artificial intelligence. This field's main goal is to let machines to perceive and understand the world similarly to humans, enabling a variety of activities like image and video processing. With time, important developments in Deep Learning for Computer Vision have come about, with the Convolutional Neural Network serving as a key approach.

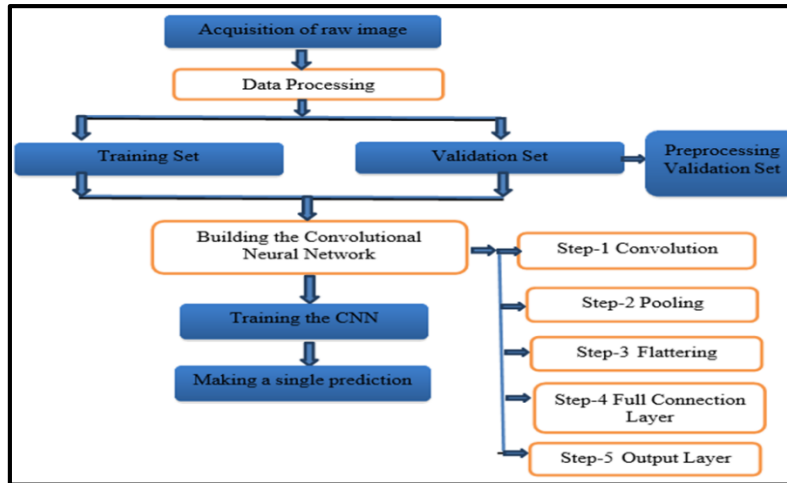


Figure 5 Methodology of CNN algorithm

A Convolutional Neural Network (ConvNet/CNN) stands as a formidable algorithm within Deep Learning, designed to process input images and allocate significance (via learnable weights and biases) to various components or objects present in the image, effectively distinguishing between them. Figure-5 shows methodology of CNN algorithm. This model is highly versatile, adept at handling one-dimensional, two-dimensional, and even three-dimensional image data. Notably, ConvNets demand considerably less pre-processing compared to alternative classification methods. Instead of manual filter engineering, ConvNets can autonomously learn these filters and characteristics through adequate training.

The architecture of a ConvNet draws inspiration from the structural layout of the Visual Cortex and mirrors the connectivity patterns observed in the Human Brain's Neurons. Individual neurons respond to stimuli within a defined region of the visual field, termed the Receptive Field. Multiple similar receptive fields are stacked together, spanning the complete visual field.

The popularity of utilizing CNNs in deep learning can be attributed to three key factors:

- CNNs alleviate the need for manual feature extraction by directly learning features, streamlining the process significantly.
- The outputs of CNNs demonstrate exceptional accuracy in recognition tasks, bolstering their effectiveness in image analysis and classification.
- CNNs are adaptable and can be retrained for new recognition tasks, allowing for the expansion and enhancement of existing networks' capabilities.

4.3. Vibration based Pothole Detection Technique

This method uses a vibration-based technology to locate potholes. Readings from smartphone sensors are used to identify instances of distress, and a special smartphone program called Sensor Logger is used for this purpose.

The accelerometer sensor used by the Sensor Logger program measures the acceleration of gravity along the x, y, and z-axes. The z-axis corresponds with vertical motion in this situation, which is often brought on by bumping into a pothole or experiencing a shift in slope. The y-axis is connected to the vehicle's turning left or right, while the x-axis represents the vehicle's acceleration and braking.

$$M = \sqrt{X^2+Y^2+Z^2}.....(1)$$

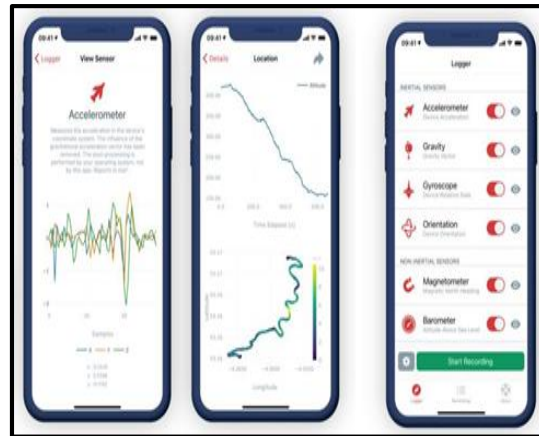


Figure 6 Sensor Logger Application

The Sensor Logger app is a free and versatile tool, which records information from various smartphone sensors, including the accelerometer, gyroscope, and GPS. An easy-to-use interface allows users to adjust the sensor selection and sampling frequency. Figure 6 shows the screen shot of sensor logger application. The app allows users to view interactive plots or export data in CSV or JSON formats. For this study, the app was used to gather data on road surface acceleration, which was then examined in Excel and graphed to show the location and severity of the distress. The graphs were used to identify major difficulties like potholes and bumps as different speeds were tested. Significant distress was indicated by peaks in the graph. Data on the minimum and average vibration helped evaluate pavement deterioration.

4.4. Manual Distress Survey

In line with IRC: 82-2015 (Code of practice for maintenance of Bituminous Road Surface), distress data on the pavement is manually gathered. Surface distress serves as a gauge of the structural and functional condition of the pavement. A proficient team of 3-4 individuals, well-trained and experienced, conducts a quantitative visual assessment of physical distress while traveling at a speed of 8-10 km/hr in a vehicle.

During the distress recording, the team visually notes and documents the following details, indicating the percentage of each category for every kilometer length i.e,Depressions/Settlements, potholes, patching, raveling, rutting.

In such situations, the pertinent data, accompanied by measurements, can be gathered on-site and documented as shown in table 1

Table 1 Data Collection sheet

Chain-age (m)		Crack s (%)	Patch Work (%)	Pothole s (%)	Bleedin g (%)	Depressi on (%)	Edge Breaking (%)	Ravelin g (%)	Rut Depth (mm)	To tal
F r o m	T o									

The rating of pavement may be assigned as per criteria given in Tables 2 to 5 for different categories of roads.

Table 2 Pavement Distress Based Rating for Highways (IRC: 82-2015)

Defects (type)	Range of Distress		
	Cracking (%)	>10	5 to 10
Patching (%)	>10	1 to 10	<1
Pothole (%)	>1	0.1 to 1	<0.1

Depression (%)	>5	1 to 5	< 1
Rut depth (mm)	>10	5 to 10	<5
Rating	1	1.1 - 2	2.1 - 3
Condition	Poor	Fair	Good

Table 3 Pavement Distress Based Rating for MDR(s) and Rural Roads

Defects (type)	Range of Distress		
Cracking (%)	>20	10 to 20	<10
Patching (%)	>20	5 to 20	<5
Pothole (%)	>1	0.5 to 1	<0.5
Depression (%)	>5	2 to 5	< 2
Rating	1	1.1 - 2	2.1 - 3
Condition	Poor	Fair	Good

Table 4 Pavement Distress Based Rating for Urban Roads

Defects (type)	Range of Distress		
Cracking (%)	>15	5 to 15	<5
Patching (%)	>1	0.1 to 1	<0.1
Pothole (%)	>5	1 to 5	< 1
Depression (%)	>10	5 to 10	<5
Rating	1	1.1 - 2	2.1 - 3
Condition	Poor	Fair	Good

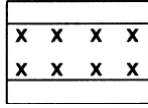
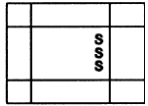
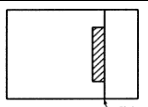
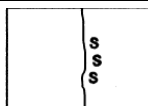
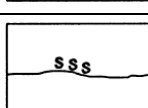
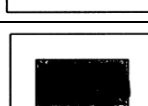



To compute the Weighted Rating Value for each specific parameter, predefined weights have been allocated (IRC: 82-2015).

Table 5 Weighted Rating

Sr. No.	Parameter	Weightage(Multiplier Factor)
1.	Cracking	1.00
2.	Patching	0.75
3.	Pothole	0.50
4.	Depression	0.75
5.	Rut depth	1.00

In the manual survey, the identified distresses were documented on sheets using the corresponding symbols denoting each type of distress. Table 6 shows types of distresses.

Table 6 Types of Distresses

Distress ID	Distress Type	Symbol
1.	Fatigue Cracking (square meters) L,M,H*	
2.	Block Cracking(square meters) L,M,H* S-Sealed	
3.	Edge Cracking(square meters)L,M,H*	
4.	Longitudinal Cracking (square meters)L,M,H*	
5.	Transverse Cracking(square meters) L,M,H*	
6.	Patch (square meters and numbers)L,M,H*	
7.	Pothole (square meters)L,M,H*	
8.	Raveling (square meters) No severity levels	
9.	Shoving (square meters) No severity levels	

*Low, Moderate and High severity levels

4.5. Present Serviceability Rating (PSR)

The Present Serviceability Rating (PSR) serves as a vital measure to evaluate the performance and condition of pavement, providing insights into its degradation and overall road damage. It heavily relies on a visual inspection method to determine the pavement's state and the severity of its degradation. In this process, inspectors use a dedicated survey form, as shown in Figure 4.5.1, employing a grading scale from 0 to 5, where 0 indicates the poorest pavement quality and 5 signifies the best.

Pavement conditions falling within grades 0 to 1 represent poor quality, exhibiting various damages and distress on high-severity road surfaces. In such cases, urgent reconstruction or rehabilitation measures are warranted. Pavements falling within grades 2 to 3 and 3 to 4 are categorized as "Fair" and "Good" conditions, respectively. For these cases, proactive maintenance is crucial to address surface problems and medium-severity issues. Conversely, a rating of 4 to 5 indicates excellent pavement condition, requiring routine maintenance to manage surface irregularities, without an immediate need for extensive maintenance.

Data for the PSR was collected through a visual examination. The Bhimpore Coastal Highway was divided into 5 segments, each approximately 7.5 meters wide and 100 meters long, to facilitate a thorough assessment of pavement condition. The official PSR values from Table 8 were utilized to accurately evaluate the pavement's condition.

Figure 7 Pavement Quality

Table 7 displays the descriptions of PSR (Present Serviceability Rating) obtained from the Highway Performance Monitoring System (HPMS) Field Manual.

Table 7 Present Serviceability Rating (PSR) ranges and descriptions

PSR	Verbal Rating	Description
0.1-1.0	Very poor	The pavement is severely degraded.
1.0-2.0	Poor	The pavement displays significant deterioration, exhibiting various damages such as raveling, cracking, and rutting, all of which significantly influence traffic speed.
2.0-3.0	Fair	Substandard riding quality, with low to medium levels of cracking and certain distress signs like patching.
3.0-4.0	Good	A smooth pavement, providing a high-quality ride, with initial signs of minimal rutting and cracking
4.0-5.0	Very good	Completely new and free from distress.

5. Data Collection

5.1. Vision based data Collection

Vision data is collected by taking pictures of the road surface with a smartphone camera in order to demonstrate the creative dynamic road pavement monitoring approach. The Convolutional Neural Network algorithm is then used to process the images that have been captured.

The road pavement surface is prone to a variety of problems, including potholes, patches, alligator cracks, longitudinal cracks, and transverse cracks. Regardless of road hierarchy or traffic volume, these damages are common on all road networks. Pavement age, traffic volume, pavement material quality, weather conditions, and asphalt erosion are the main causes of these damages. The data collection took place in sunny weather, which provided ideal conditions for monitoring the condition of the road pavement.

5.2. Vibration based Data Collection

A smartphone app called Sensor Logger is used to collect vibration data from the pavement surface. This application measures acceleration data using the smartphone's accelerometer sensor. It also records location information, including latitude and longitude. The application provides thorough vibration data for analysis by gathering sensor data at a rate of 10 readings per second. Figure 8 shows a screen shot of spreadsheet containing recorded Acceleration data.

Distance	z	Y	X	15km/h	Distance	z	Y	X	20 km/h	Distance	Z	Y	X	25 km/h	
0	7.605	0.04605	4.66605	8.922454	0	9.538951	-0.66405	-2.586	9.905551	0	10.55205	-0.09195	-0.18495	10.55407	
	8.941051	-0.13695	3.06	9.451177		9.69495	0.87405	-1.70505	9.88247		11.454	-1.02495	-2.74605	11.82309	
	7.938	-0.444	4.28295	9.03065		10.923	-0.02295	-0.31395	10.92754		8.38095	0.02205	-3.579	9.11318	
	8.509951	-0.82695	3.62895	9.288293		10.27905	0.084	-0.657	10.30037		5.61405	-0.74295	-3.79995	6.819762	
	8.802	-0.48	3.47805	9.476415		7.87305	-1.06605	-3.02895	8.502701		8.818951	1.27605	-1.95705	9.12317	
	7.33695	-0.63795	2.80095	7.879286		10.52805	0.252	-1.72395	10.67124		7.94295	0.03405	-1.97295	8.184385	
	7.72695	0.30405	3.41595	8.453811		10.35495	0.11295	-0.56805	10.37114		11.538	0.09405	-0.171	11.53965	
	8.79	0.25695	3.41895	9.435006		10.18095	-0.45795	-0.10095	10.19174		8.11695	0.82095	-3.24705	8.780784	
	9.27795	0.048	2.77005	9.68276		7.88505	-0.05595	-1.878	8.105802		8.82795	0.52005	-3.06	9.357711	
	8.685	-0.10395	2.949	9.172603		8.835	-1.329	-2.99805	9.424		9.28995	-0.90795	-1.66695	9.481892	
	9.901051	-0.702	2.98305	10.36447		12.03795	0.74205	-1.13595	12.11418		6.693	0.843	-3.88605	7.785133	
	9.870001	-0.75495	2.049	10.10867		10.329	-0.29805	0.88605	10.37122		10.12095	0.70395	-0.16395	10.14673	
	10.209	-0.645	1.54695	10.34566		9.27795	-0.18795	-2.36595	9.576712		11.313	-0.525	-0.82695	11.35533	
	10.60695	-0.3	1.18095	10.67671		8.44095	-0.94905	-2.06895	8.742476		9.20205	0.33105	-2.81805	9.629576	
	10.035	-1.31505	1.37895	10.21431		11.02305	0.36405	-0.34095	11.03433		10	8.95005	1.11795	-3.711	9.753191
	7.507051	-0.171	2.23095	7.833402		10.84395	0.97005	0.462	10.89705		8.59605	-0.11595	-4.72605	9.810254	
	8.842951	-1.69305	2.61705	9.376201		10.236	0.15795	-0.252	10.24032		9.76051	-0.01305	-1.59705	9.898742	
	7.773	-0.94605	3.849	8.725213		8.467051	0.58005	-1.533	8.624239		10.72905	0.72105	-2.24895	10.98591	
	8.682	-0.465	3.057	9.216214		9.415051	-0.35805	-1.96605	9.624798		11.631	0.26805	-1.22205	11.6981	

Figure 8 A spreadsheet containing recorded Acceleration Data

5.3. Data collection using Bike, Car & Manual (Visual)

To record vibration data, a smartphone of the 'Activa 6G' model was safely mounted on the top side of a bike as shown in figure 9. This information was gathered in February 2022 during the daytime at various speeds of 15 km/h, 20 km/h, and 25 km/h. As the vehicle moved, the application measured the actual length of the road segment. Five monitoring iterations were carried out for each travel speed along the street segment in order to improve vibration measurements, with the goal of determining the most precise number of iterations.



Figure 9 Mobile Mounted on Bike and Car

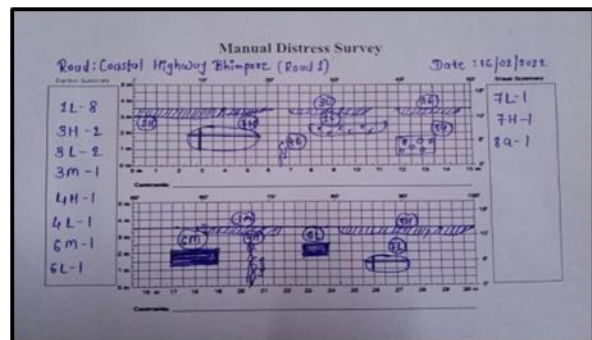


Figure 10 Manual Measurement of distress

Figure 11 Manual Distress Survey Sheet based

A smartphone was attached to the dashboard of the vehicle, a 'Honda Amaze' model, using a typical mobile handle, as shown in figure 9 Data was measured and collected in March 2022, also in the daytime as shown in figure 10 and 11.

Five iterations at each of three different travel speeds (15, 20, and 25 km/h) were used. During the data collection process, the start and end points of both vehicle modes were predetermined locations on the road.

To evaluate physical distress shown in figure 10, a skilled team of 3-4 individuals with ample experience and training conducted a quantitative visual assessment while walking on the road surface. Additionally, a survey form for Present Serviceability Rating was completed during the manual distress survey. Data Analysis

5.4. Analysis of Data Collected using Vision Method

We chose five road segments, each 100m long, to compare the vibration-based and vision-based approaches. In this study, we used a smartphone camera to take pictures of the road surface along all five stretches. From each stretch, 10 images were taken, yielding 50 total images. With the help of a Convolutional Neural Network (CNN), we were able to identify potholes in images by classifying them as "Pothole" in predictions and "Normal" in predictions for images without potholes. A manual distress survey of all images was used to verify the validity of these predictions. Table 8 shows vision based data analysis.

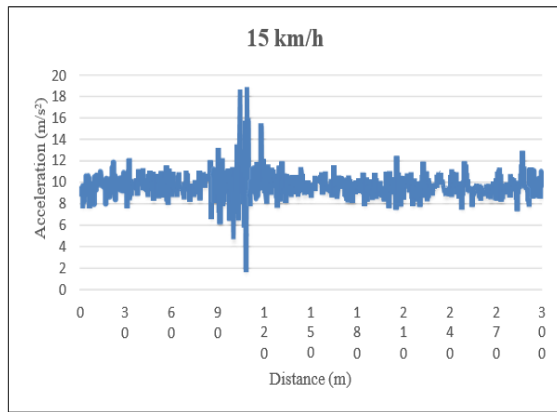
Table 8 Vision based Data Analysis

No. of potholes									
Road 1		Road 2		Road 3		Road 4		Road 5	
Image No.	Prediction	Image No.	Prediction	Image No.	Prediction	Image No.	Prediction	Image No.	Prediction
1.	Normal	1.	Normal	1.	Normal	1.	Normal	1.	Normal
2.	Pothole	2.	Normal	2.	Normal	2.	Normal	2.	Normal
3.	Pothole	3.	Pothole	3.	Normal	3.	Normal	3.	Normal
4.	Normal	4.	Pothole	4.	Normal	4.	Pothole	4.	Pothole
5.	Pothole	5.	Pothole	5.	Normal	5.	Pothole	5.	Pothole
6.	Normal	6.	Pothole	6.	Normal	6.	Pothole	6.	Pothole
7.	Normal	7.	Normal	7.	Normal	7.	Pothole	7.	Pothole
8.	Normal	8.	Normal	8.	Normal	8.	Pothole	8.	Normal
9.	Normal	9.	Normal	9.	Pothole	9.	Normal	9.	Normal
10.	Normal	10.	Normal	10.	Pothole	10.	Normal	10.	Normal

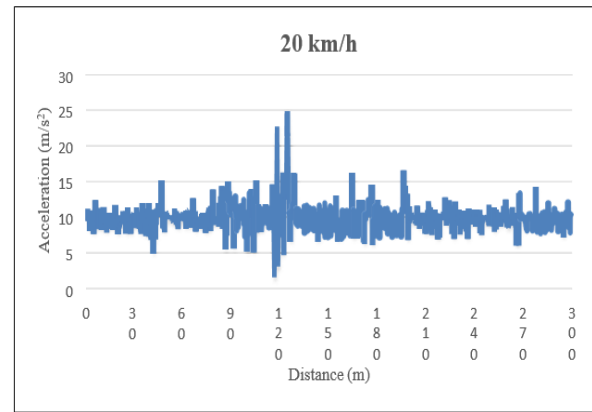
5.5. Analysis of Data Collected using Vibration Method

The graph shows how much the pavement vibrates when a 'bike' is moving at different speeds figure 12. The slow bike movement causes slight vibration changes at 15 km/h. Average vibrations ranged from 1.873 m/s² to 18.874 m/s², respectively. The highest and lowest average vibrations were 26.228 m/s² and 1.683 m/s² at 20 km/h, respectively. These values were 30.998 m/s² and 3.551 m/s² at 25 km/h.

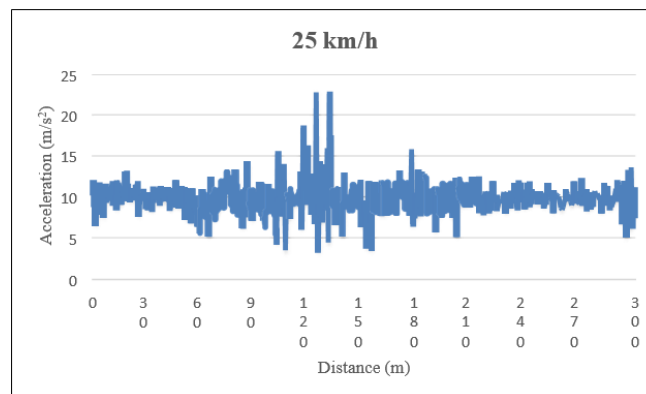
Vibration damages pavement and increases with speed. Smartphone sensors exhibit high sensitivity to vibrations from moving traffic. Higher bike speeds increase the precision of vibration data, revealing serious pavement damage like potholes. Lower vibration values, however, imply that maintenance is not immediately required.



Magnitude of pavement vibration data at speed of 15 km/h



Magnitude of pavement vibration data at speed of 20 km/h

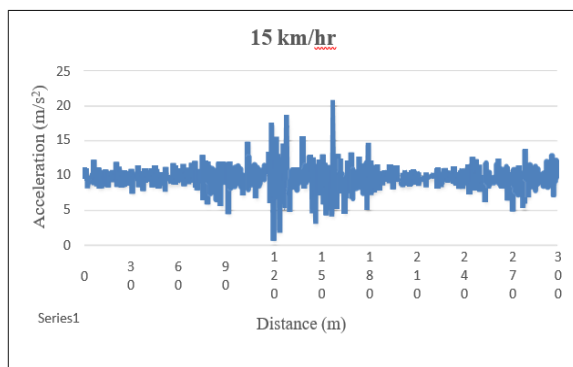


Magnitude of pavement vibration data at speed of 25 km/h

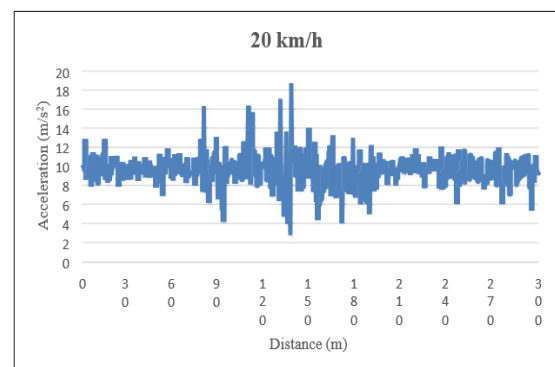
Figure 12 Analysis of data collected using BIKE at different Speed

Significant variations can be seen in the figures, which show pavement vibration data obtained from the ‘car’ at various speeds figure 13. The vibration levels varied from about 0.904 m/s² at 15 km/h to about 20.81 m/s² at a speed that reflected the car's slow motion. The highest and lowest values were 25.51 m/s² and 2.15 m/s², respectively, at 20 km/h. The maximum vibration data at 25 km/h was around 26.84 m/s², and the minimum was about 0.567 m/s².

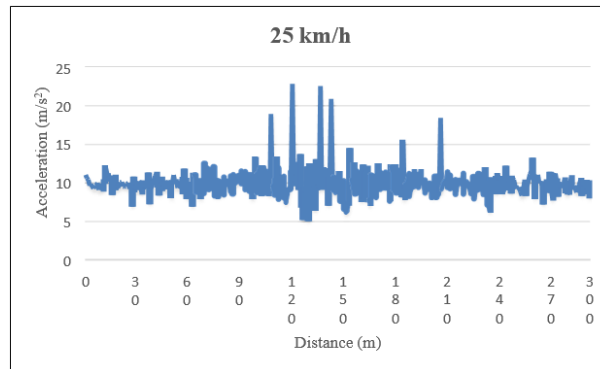
Due to the smartphone sensor's increased sensitivity, it is notable that speeds of 15 km/h and 25 km/h show a significant variation between maximum and minimum vibration data. The results highlight a direct correlation between pavement vibration measurements and travel speeds, with higher speeds causing more pavement vibration because of amplified vibrations in the vehicle chassis.



Magnitude of pavement vibration data at speed of 15 km/h



Magnitude of pavement vibration data at speed of 20 km/h



Magnitude of pavement vibration data at speed of 25 km/h

Figure 13 Analysis of data collected using CAR at different Speed

5.6. Factors Influencing Distress Detection Accuracy

- Vehicle Speed
- Vehicle Type
- Vehicle Age
- Number of Iterations
- Vehicle Condition

5.7. Comparison of data collected using Bike and Car

Following manual surveying, it is evident that pavement vibration data collected by bike is most accurate at 25 km/h, while data collected by car is most accurate at 20 km/h. As a result, it is possible to conclude that the pavement vibration data obtained via the smartphone application in both vehicle tests is of sufficient accuracy. Figure 14 shows comparison of data collected using bike and car.

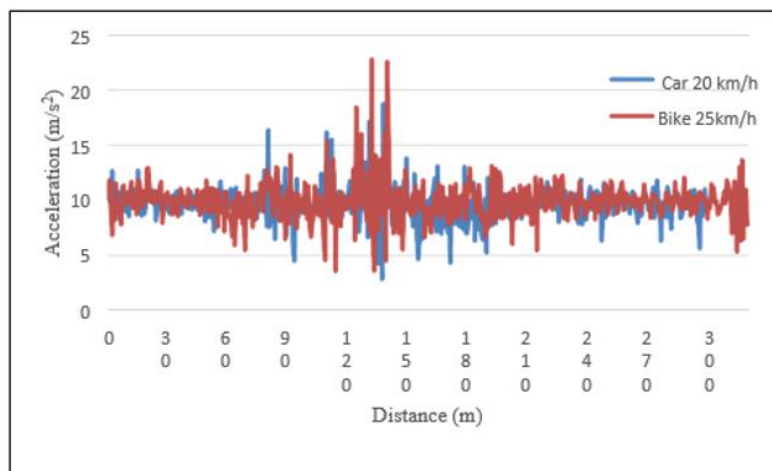


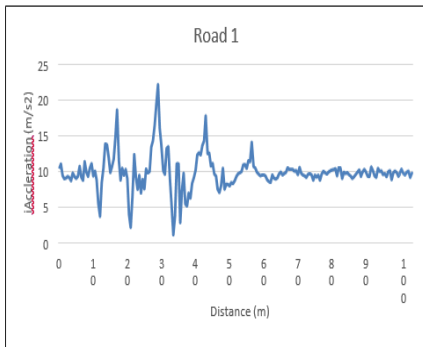
Figure 14 Comparison of data collected using Bike and Car

The study reveals that the highest acceleration vibration is observed between 90m and 150m, indicating significant road distress, likely major types like potholes and alligator cracks, requiring immediate maintenance. Less fluctuation is observed from 150m to 180m, suggesting minor distress like patches and cracks. The method provides accurate distress location but doesn't precisely identify distress types. The experiment highlights the suitability and accuracy of both bikes and cars for pavement monitoring, and the significant influence of travel speed on pavement vibration data precision.

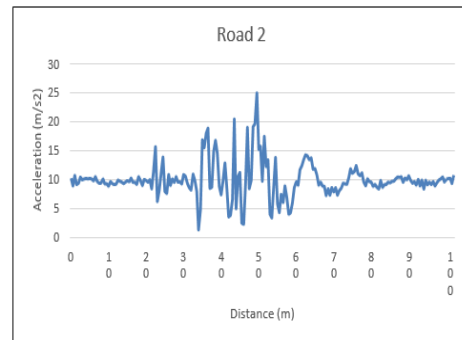
5.8. Data Analysis of five road stretches collected using Car

Data analysis using both a bike and a car confirmed that both vehicles are suitable and precise as test vehicles for pavement monitoring. Previous research highlighted the accuracy of data collection at 20 km/h using the Honda Amaze car. As a result, for data collection across the five road segments, the Honda Amaze car was driven at a speed of 20 km/h.

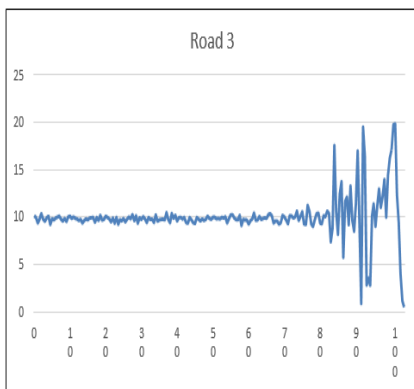
We chose five 100m road stretches to compare vibration and vision-based methods. On all five roads, the Sensor Logger application was used to collect acceleration data from the road surface. This acceleration data was then meticulously analysed in Excel. The number of potholes was determined using the resulting Excel-generated graph. Manual distress surveys were used to validate the accuracy of this analysis. Figure 15 shows Magnitude of pavement vibration on all the roads



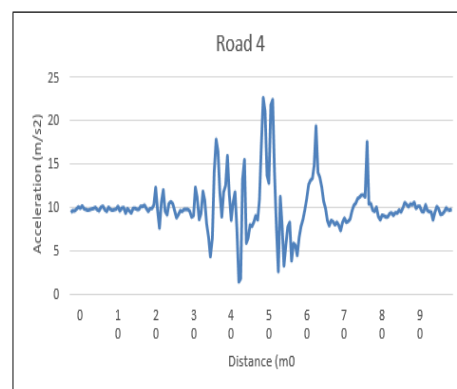
Magnitude of pavement vibration data of road 1



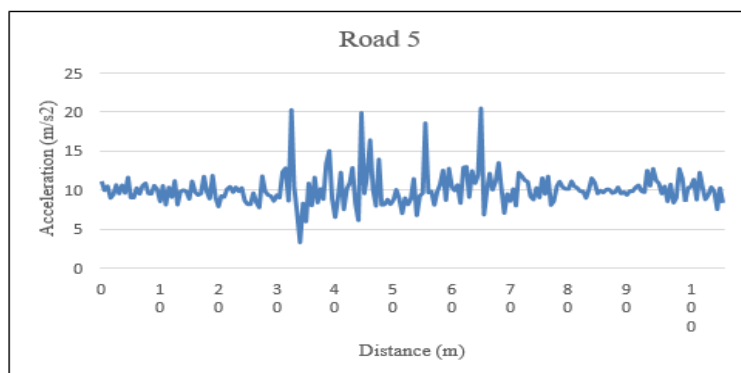
Magnitude of pavement vibration data of road 2



Magnitude of pavement vibration data of road 3



Magnitude of pavement vibration data of road 4



Magnitude of pavement vibration data of road 5

Figure 15 Magnitude of pavement vibration on all the roads

The summary of all collected data have been mentioned in table 9, table 10, table 11 and table 12

Table 9 No. of Distress Calculation using vibration method

RoadNo.	Major Distress like Pothole	Minor Distress
1.	3	1
2.	3	3
3.	3	0
4.	4	2
5.	4	0

5.9. Analysis of data collected using Manual Method

Name of the Road: Coastal Highway Bhimpore Distance: 1 km

Type of Surface: Flexible Pavement Carriage Width: 7.0m

Date of Observation: 13/03/2022 Weather Condition: Hazy Sunshine

Table 10 Manual Data Collection

Chain age(m)		Cracks (%)	PatchWork (%)	Potholes(%)	Depression \varnothing	Rut Depth (mm)	Total
From	To						
0	100	15	10	0	0	0	25
100	200	7	0	25	0	0	32
200	300	5	0	0	0	0	5
300	400	25	15	0	5	10	45
400	500	10	10	5	0	0	25
500	600	35	0	14	7	15	71
600	700	30	4	0	5	15	54
700	800	13	0	3	0	0	16
800	900	28	30	16	9	10	93
900	1000	22	25	20	0	0	67

Table 11 Manual Data Collection for length 1 Km

Chain age(m)		Cracks (%)	Patch Work (%)	Potholes (%)	Depression \varnothing	Rut Depth (mm)	Total
From	To						
0	1000	19	9.4	8.3	2.6	5	44.3
Rating as per Table 12		1	1	1	1.5	2.0	
Condition		Poor	Poor	Poor	Fair	Fair	

Table 12 Final Rating Calculation

Distress Type	Rating as per Table 4.2	Weightage as per Table 4.5	Weighted Rating Value
Cracking	1.0	1.00	1.0
Patching	1.0	0.75	0.75
Pothole	1.0	0.50	0.50
Depression	1.5	0.75	1.13
Rut depth	2.0	1.00	2.0
Final Rating Value			1.07
Road Condition			Poor

5.10. No. of potholes on five road stretches

To compare vibration and vision-based methods, we selected five road stretches, each spanning 100m. We also conducted a manual distress survey on these roads. The number of potholes on each of the five stretches was determined through careful manual observation of the road condition. The table 13 below provides the count of potholes observed on these stretches. Table 14 shows PSR rating of five road stretches.

Table 13 No. of potholes calculation using Manual Method

Road 1	Road 2	Road 3	Road 4	Road 5
3	4	3	5	4

Table 14 PSR rating of five road stretches

Road No.	PSR	Verbal Rating
1.	1.0	Poor
2.	1.1	Poor
3.	2.5	Fair
4.	0.5	Very Poor
5.	1.2	Poor

6. Validation and Comparison of Results

Both experiments were conducted on identical stretches of road to compare the effectiveness of pothole detection methods using vibration and vision. For this study, we chose five road segments that were each 100m long. We validated both methods further by cross-referencing them with manual surveys.

Acceleration data for the vibration-based method was collected using a car along a 100m stretch of road during the comparison process. To implement the vision-based approach, photographs of the road surface were taken along the same 100m stretch for all five roads at the same time. The accuracy of each method in identifying different types of distress was quantified and compared.

A manual distress survey was conducted on the study road stretch to validate the results. The vibration-based method used graphs plotted in Excel to determine distress locations. The vision-based method identified distress locations based on the latitude and longitude data associated with images collected using the smartphone's GPS. The results of the manual distress surveys were then compared to the locations of distress identified using both vibration and vision-based methods as shown in Table 16

Table 15 Rating of potholed based on three techniques

Rating for No. of Potholes			
Road No.	Vision based method	Vibration based method	Manual Method
1.	3	3	3
2.	4	3	4
3.	2	3	3
4.	5	4	5
5.	4	4	4

The accuracy in detecting potholes using both the methods is also compared and shown in Table 16

Table 16 Accuracy of detection of individual distresses: vibration vs. vision method

Distress	Vision based method (%)	Vibration based method (%)
Pothole	90	80

The results show that the vibration-based method detects potholes with an 80% accuracy. Variations in pavement vibration data are influenced by factors such as vehicle type, vehicle speed, and smartphone position, according to the study. The vibration-based method's accuracy is limited because it can only detect distresses along the wheel path.

The vision-based method, on the other hand, achieves higher accuracy due to its wider field of view. Unlike the vibration-based method, the vision-based approach not only pinpoints the location of the distress but also allows for more precise identification of the type of distress.

7. Conclusion

While both methods are cost-effective and accurate, the vision-based approach is more effective than the vibration-based method, which is limited to detecting distress along the wheel path.

The vibration-based pothole detection method locates distress accurately but cannot precisely identify the type of distress.

Vibration-based pothole detection can be performed at any time of day or night, whereas image processing for the vision-based method necessitates adequate lighting, particularly at night.

The vibration-based method is faster than the vision-based method because image processing requires more calculations and thus takes longer.

Despite its lower accuracy, the vibration-based method is appropriate for gathering general pavement condition data, whereas the vision-based method is best suited for precise maintenance work.

Although automated techniques such as vibration-based and vision-based analyses can provide an initial assessment of the pavement's condition, they cannot completely replace traditional.

Compliance with ethical standards

Disclosure of conflict of interest

No conflict of interest to be disclosed.

References

- [1] AbhayTawalare K, Vasudeva Raju, Pavement Performance Index for Indian rural roads, Elsevier 2016.
- [2] Ahmet Bahaddin Ersoz, Onur Pekcan and Turker Teke, "Crack identification for rigid pavements using unmanned aerial vehicles", IOP Conf. Series: Materials Science and Engineering 236 (2017) 012101.
- [3] Amir Shtayat , Sara Moridpour, Berthold Best, Using e-bikes and private cars in dynamic road pavement monitoring, International Journal of Transportation Science and Technology, 2021.
- [4] Amir Shtayat,, Sara Moridpour, Berthold Best, Avinash Shroff, Divyajeetsinh Raol, "A review of monitoring systems of pavement condition in paved and unpaved roads", Journal of Traffic & Transportation Engineering, 2020.
- [5] Amjad Issa, Haya Samaneh,, Mohammad Ghanim, "Predicting pavement condition index using artificial neural networks approach", Ain Shams Engineering Journal, 2021.
- [6] Antonella Ragnoli, Maria Rosaria De Blasiis and Alessandro Di Benedetto, "Pavement Distress Detection Methods: A Review", Infrastructures (2020).
- [7] Anurag Sinha, Pratik Hagawane, "Method Comparison of Pavement Condition Rating based on IRC & ASTM Guidelines", International Research Journal of Engineering and Technology (IRJET), 2020.
- [8] Bayu Setiawan, Ary Setyawan and Budi Yulianto, "The Development of Road Evaluation and Monitoring System Using Database Application", AIP Conference Proceedings 2114, 060014 (2019).
- [9] Brahim Benmhahe, Jihane Alami Chentoufi, "Automated Pavement Distress Detection, Classification and Measurement: A Review", (IJACSA) International Journal of Advanced Computer Science and Applications 2021.
- [10] Ce Zhang, Ehsan Nateghinia, Luis F. Miranda-Moreno, Lijun Sun, "Pavement distress detection using convolutional neural network (CNN): A case study in Montreal, Canada", International Journal of Transportation Science and Technology, 2021.
- [11] Chun-Hsing Ho, Matthew Snyder, Dada Zhang, "Application of Vehicle-Based Sensing Technology in Monitoring Vibration Response of Pavement Conditions", American Society of Civil Engineers, 2020.
- [12] Distress Identification manual for the Long Term Pavement Performance Program (U S Department of Transportation, Federal Highway Administration
- [13] Douangphachanh and Oneyama EURASIP Journal on Wireless Communications and Networking 2014.
- [14] Eldor Ibragimov, Hyun-Jong Lee, Jong-Jae Lee and Namgyu Kim, "Automated pavement distress detection using region based convolutional neural networks" International Journal of Pavement Engineering, 2020.
- [15] G. Srinidhi and Renuka Devi S M, "Pothole Detection using CNN and AlexNet", International Conference on Communication and Information Processing (ICCIP- 2020).
- [16] Hua-Ping Wang, Ping Xiang and Li-Zhong Jiang, "Optical fiber sensing technology for full-scale condition monitoring of pavement layers", Road Pavement and Material Design, 2018.
- [17] IRC 82- 2015 Code of Practice for maintenance of Bituminous Road Surface
- [18] IRC:SP:83-2018 Guidelines for Maintenance Repari and rehabilitation of Cement Concrete Pavement
- [19] Janani Lekshmiathy, Nisha M.Samuel, Sunitha Velayudhan, "Vibration vs. vision: best approach for automated pavement distress detection", International Journal of Pavement Research and Technology, 2020.
- [20] Lucia Rusu, Dan Andrei Sitar Taut, Sergiu Jecan, "An Integrated Solution for Pavement Management and Monitoring Systems", 22nd International Economic Conference – IECS 2015 "Economic Prospects in the Context of Growing Global and Regional Interdependencies", IECS 2015.
- [21] M J Chin, P Babashamsi and N I M Yusoff, "A comparative study of monitoring methods in sustainable pavement management system", 10th Malaysian Road Conference & Exhibition 2018.
- [22] M. N. Nagabhushana, "Pavement Testing: Accelerated Pavement Testing", New Building Materials and Construction World, New Delhi, 2019.
- [23] Markus Eisenbach, Ronny Stricker, Daniel Seichter, Karl Amende, Klaus Debes, Maximilian Sesselmann, Dirk Ebersbach, Ulrike Stoeckert , and Horst-Michael Gross, "How to Get Pavement Distress Detection Ready for Deep Learning? A Systematic Approach", Int. Joint Conf. on Neural Networks (IJCNN), Anchorage, USA, 2017.

- [24] Preset Serviceability Rating Computation from Reported Distresses FHWA-HRT-21-041
- [25] Prof. Dr Fareed M.A. Karim, Dr Khaled Abdul Haleem Rubasi, and Dr Ali Abdo Saleh, “The Road Pavement Condition Index (PCI) Evaluation and Maintenance: A Case Study of Yemen”, *Organization, Technology and Management in Construction* 2016; 8: 1446–1455.
- [26] Ronald Roberts, Laura Inzerillo and Gaetano Di Mino, “Using UAV Based 3D Modelling to Provide Smart Monitoring of Road Pavement Conditions”, *Information* 2020.
- [27] Sumarwan, Sri Sunarjono, Agus Riyanto and Nurul Hidayati, “Development of Road Condition Database Based on Geographical Information System and Pavement Condition Index Method”, *AIP Conference Proceedings* 2114, 020004 (2019).
- [28] Sunil G, Yateen Lokesh , Nikhil T, “Pavement Serviceability Index for Urban Roads in Bengaluru”, *International Journal of Innovative Science and Research Technology*, 2018.
- [29] Sunil Kumar Sharma, Haidang Phan and Jaesun Lee, “An Application Study on Road Surface Monitoring Using DTW Based Image Processing and Ultrasonic Sensors”, *Applied Science Article*, 2020.
- [30] T Arianto, M Suprpto and Syafi, “Pavement Condition Assessment Using IRI from Roadroid and Surface Distress Index Method on National Road in Sumenep Regency”, *International Conference on Advanced Materials for Better Future* 2017.
- [31] Teng Wang, Kasthurirangan Gopalakrishnan, Omar Smad, Arun K. somani, “Automated Shape-Based Pavement Crack Detection Approach”, *TRANSPORT* ISSN 1648-4142/eISSN 1648-3480 2018 Volume 33 Issue 3: 598–608.
- [32] Viengnam Douangphachanh and Hiroyuki Oneyama, “A study on the use of smartphones under realistic settings to estimate road roughness condition”,
- [33] Vinicius M.A. Souza, “Asphalt pavement classification using smartphone accelerometer and Complexity Invariant Distance”, *Engineering Applications of Artificial Intelligence*, 2018.
- [34] Wanli Ye, Wei Jiang, Zheng Tong, Dongdong Yuan, Jingjing Xiao, “Convolutional neural network for pothole detection in asphalt pavement”, *Road Materials and Pavement Design*, 2019.
- [35] Wenjing Xue, Dong Wang, Linbing Wang, “A Review and Perspective about Pavement Monitoring”, *ISSN Chinese Society of Pavement Engineering*, 2012.
- [36] Yifan Pan, Xianfeng Zhang, Guido Cervone, and Liping Yang, “Detection of Asphalt Pavement Potholes and Cracks Based on the Unmanned Aerial Vehicle Multispectral Imagery”, *IEEE journal of selected topics in applied earth observations and remote sensing*.
- [37] Yogesh U. Shah, Dr. S.S.Jain, Devesh Tiwari, Dr. M.K. Jain, “Analysis of Flexible Pavement Serviceability Using ANN for Urban Roads”, *Airfield and Highway Pavement 2013: Sustainable and Efficient Pavements* © ASCE 2013